Biodesign

pISSN 2288-6982 | eISSN 2288-7105

CRYSTALLIZATION P 114-117

Purification, crystallization, and X-ray crystallographic analysis of Vac8p complexed with Atg13p from *Saccharomyces cerevisiae*

Jumi Park[1,4], Kyonghwa Song[2], Sohyeon Oh[2], Taewon Son[2], Jun Lee[2], Ayoung Park[2], Hyun Ji Kim[2], Youngsoo Jun[3,4] and Changwook Lee[1,4]*

[1]Department of Biological Sciences, School of Life Sciences, Ulsan National Institute of Science and Technology, 50 UNIST-gil, Ulsan 44919, Republic of Korea, [2]Busan Science High School, 455-1 Geumsaem-ro, Busan 46235, Republic of Korea, [3]School of Life Sciences and [4]Cell Logistics Research Center, Gwangju Institute of Science and Technology, Gwangju 61005, Republic of Korea.
*Correspondence: changwook@unist.ac.kr

Vac8p is a vacuolar protein that plays pivotal roles in both vacuole inheritance and the formation of nucleus vacuole junction (NVJ) in yeast. The Vac8p directly interacts with Atg13p, a component of the autophagy machinery, and mediates cytoplasm-to-vacuole targeting (Cvt) pathway, resulting in the maturation of aminopeptidase I (Ape1p). Here, we co-expressed and purified *Saccharomyces cerevisiae* Vac8p complexed with Atg13p in *Escherichia coli* bacteria cells, and crystallized the complex proteins under the condition of 25% (v/v) PEG 400, 100 mM Tris pH 8.5, 2% (v/v) Ethylene glycol, 2% (w/v) PEG 3350, 1.5% (w/v) PEG 20000, 5 mM DTT at 293K. X-ray diffraction data of the crystals were collected to 2.9 Å resolution at the synchrotron radiation. The crystals belong to the orthorhombic space group $P2_12_12_1$ with unit cell parameters a = 62.7 Å, b = 92.4 Å, and c = 139.9 Å. The asymmetric unit contains one Vac8p-Atg13p heterodimer with a corresponding V_M of 2.92 Å^3 Da^{-1} and solvent content of 57.8%.

INTRODUCTION

Vac8p, vacuolar protein 8, is a 64 kDa vacuolar membrane protein comprising 12 armadillo (ARM) repeats across its whole sequence (Tewari et al., 2010). Vac8p plays an essential role in vacuole inheritance through direct interaction with Vac17p-Myo2p complex (Ishikawa et al., 2003; Tang et al., 2003). Vac8p also directly interacts with Nvj1p, an outer nuclear membrane protein, and mediates nucleus-vacuole junction (NVJ), which has been well characterized as a membrane contact site (MCS) (Roberts et al., 2003). In addition, two-hybrid and co-immunoprecipitation studies have identified that Vac8p associates with Atg13p. This Vac8p-Atg13p interaction is critical for recruiting of Atg1p complex to the pre autophagosomal structure (PAS) during the cytosol-to-vacuole targeting (Cvt) pathway to eventually transport aminopeptidase I (Ape1p) into vacuoles (Scott et al., 2000; Torggler et al., 2016; Wang et al., 1998). Most vacuole-resident hydrolases are transported into the vacuole through the conventional secretory and endocytic pathways (Klionsky et al., 1990; Riezman, 1985; Takeshige, 1992), while Ape1p is synthesized as an inactive precursor (preApe1p) in the cytoplasm, and directly transferred into vacuoles, where preApe1p matures upon the cleavage of the propeptide (Klionsky, 1992). Vac8p mutants defective for interaction with Atg13p accumulate preApe1p in the cytoplasm, indicating that both Vac8p and Atg13p are required to transport preApe1p into vacuoles (Scott et al., 2000). Atg13p has been known as a regulatory subunit of the Atg1p signaling complex. In particular, Atg13p is involved in vesicle formation during autophagy by stimulating Atg1p kinase activity (Funakoshi et al., 1997).

Previous studies have shown that Vac8p-Atg13p interaction is mediated by the armadillo repeats of Vac8p (Scott et al., 2000). Recently, we reported the crystal structure of Vac8p in complex with Nvj1p at 2.4 Å resolution (Jeong et al., 2017). The structural studies combined with biochemical experiments have shown that the interaction between Vac8p-Atg13p might highly resemble that shown in Vac8p-Nvj1p, and that Atg13p competes with Nvj1p for the interaction with Vac8p (Jeong et al., 2017). However, the molecular details by which Vac8p might specifically recognize Atg13p and eventually mediate Cvt pathway remain unclear. In this study, we co-expressed and purified Vac8p-Atg13p complex, and crystallized the complex using PEG 400 as a precipitant solution. We successfully obtained X-ray diffraction data for the complex at 2.9 Å resolution.

RESULTS AND DISCUSSION

Initially, we tried to purify full-length Vac8p (residues 1 to 578) in complex with a C-terminal fragment of Atg13p (residues 567 to 738). However, the C-terminus of Atg13p was easily degraded during protein purification for unknown reasons. Previous studies involving limited proteolysis revealed that truncated form of Vac8p comprising residues 10 to 515 is the most stable fragment

(Jeong et al., 2017). Therefore, we generated constructs of Vac8p (residues 10 to 515) and C-terminally truncated Atg13p (residues 567 to 695), and co-expressed them using BL21 (DE3) *E. coli* bacterial cells (Table 1 and 2). The complex was purified to homogeneity, and the purity of Vac8p-Atg13p in the final purification step was at least 96% as monitored by SDS-PAGE. Size-exclusion chromatography confirmed that the truncated form of Vac8p still retained the ability to interact with the truncated Atg13p (Figure 1). The initial crystals of Vac8p-Atg13p complex grew to maximum dimensions of 0.02 x 0.02 x 0.5 mm in five days. However, the crystals diffracted X-ray only up to 6–7 Å resolution at the synchrotron radiation. To get crystals of high diffraction quality, we used Additive Screen kit (Hampton Research), and finally obtained crystals capable of diffracting to a maximum of 2.9 Å resolution under the condition of 25% (v/v) PEG 400, 100 mM Tris pH 8.5, 2% (v/v) Ethylene glycol, 2% (w/v) PEG 3350, 1.5% (w/v) PEG 20000, 5 mM DTT at 293K (Figure 2, Table 3). X-ray diffraction data were collected with 95.2% completeness at the 5C beamline at Pohang Accelerator Laboratory (Pohang, Republic of Korea) (Figure 3) (Park et al., 2017). Crystals belong to the orthorhombic space group $P2_12_12_1$ with unit cell parameters of a = 62.7 Å, b = 92.4 Å, c = 139.9 Å and $\alpha = \beta = \gamma = 90^{\circ}$. The asymmetric unit contains one Vac8p-Atg13p heterodimer with a corresponding V_M of 2.92 $Å^3$ Da^{-1} and solvent content of 57.8% (Matthews, 1968) (Table 4). Currently, we are solving the structure of Vac8p-Atg13p complex by molecular replacement method using the Vac8p-Nvj1p complex structure (PDB entry 5XJG) as a search model.

METHODS

Cloning and Overexpression

The full-length Vac8p gene was amplified from *S. cerevisiae* genomic DNA using PCR. The amplified gene was digested with restriction enzymes, BamHI (N-terminus) and SalI (C-terminus), respectively. The digested fragment was ligated into pGEX-6p1 vector (GE Healthcare). The construct encodes N-terminal GST, followed by a PreScission protease recognition site (Leu-Glu-Val-Leu-Phe-Gln/Gly-Pro) and Vac8p. Gene encoding *S. cerevisiae* Atg13p (567-738) was amplified using PCR. The PCR product was cloned into pCDFDuet-1 vector with an N-terminal hexa-histidine tag prior to a tobacco etch virus (TEV) protease cleavage site and Atg13p. Each plasmid was isolated and co-transformed into an *Escherichia coli* BL21 (DE3) expression strain (Table 1 and 2). Vac8p-Atg13p proteins were expressed by induction with 0.3 mM isopropyl β-D-1-thiogalactopyranodise (IPTG), when the cell density reached an OD_{600} value of ~ 0.6. Cells were further incubated for 18 hours at 18 ˚C with vigorous shaking, and were harvested by centrifugation at 4,000 rpm for 15 min at 4˚C. They were then resuspended in buffer comprising 25 mM sodium phosphate, pH 7.8, 400 mM NaCl, and 10 mM imidazole.

Purification of Vac8p-Atg13p protein complex

Vac8p-Atg13p complex was purified using Ni^{2+}-immobilized metal affinity chromatography (Ni^{2+}-IMAC). The sonicated lysed cells were applied to

TABLE 1 | Vac8p production information

Source organism	*Saccharomyces cerevisiae* S288C
DNA source	*Saccharomyces cerevisiae* S288C genomic DNA
UniProt ID	P39968
Forward primer	GCCGGATCCGATTCTTCAGACGAGGCC
Reverse primer	GCCGTCGACTCATTTTCTCACTCCGTTAAT
Cloning vector	pGEX-6p-1
Expression host	*E. coli* BL21(DE3)
Complete amino acid sequence of the construct produced	DSSDEASVSPIADNEREAVTLLLGYLEDKDQLDFYSGGPLK ALTTLVYSDNLNLQRSAALAFAEITEKYVRQVSREVLEPILI LLQSQDPQIQVAACAALGNLAVNNENKLLIVEMGGLEPLIN QMMGDNVEVQCNAVGCITNLATRDDNKHKIATSGALIPLT KLAKSKHIRVQRNATGALLNMTHSEENRKELVNAGAVPVL VSLLSSTDPDVQYYCTTALSNIAVDEANRKKLAQTEPRLVS KLVSLMDSPSSRVKCQATLALRNLASDTSYQLEIVRAGGLP HLVKLIQSDSIPLVLASVACIRNISIHPLNEGLIVDAGFLKPLV RLLDYKDSEEIQCHAVSTLRNLAASSEKNRKEFFESGAVEK CKELALDSPVSVQSEISACFAILALADVSKLDLLEANILDAL IPMTFSQNQEVSGNAAAALANLCSRVNNYTKIIEAWDRPN EGIRGFLIRFLKSDYATFEHIALWTILQLLESHNDKVEDLVK NDDDIINGVRK

TABLE 2 | Atg13p production information

Source organism	*Saccharomyces cerevisiae* S288C
DNA source	*Saccharomyces cerevisiae* S288C genomic DNA
UniProt ID	Q06628
Forward primer	GCCGGATCCGGTGGGAATTCATCTACT
Reverse primer	GCCGTCGACTTAACCATTATCGATTAACTTATT
Cloning vector	pCDFDuet-1
Expression host	*E. coli* BL21(DE3)
Complete amino acid sequence of the construct produced	GGNSSTSALNSRRNSLDKSSNKQGMSGLPPIFGGESTSYHH DNKIQKYNQLGVEEDDDDENDRLLNQMGNSATKFKSSISP RSIDSISSSFIKSRIPIRQPYHYSQPTTAPFQAQAKFHK PANKLIDNG

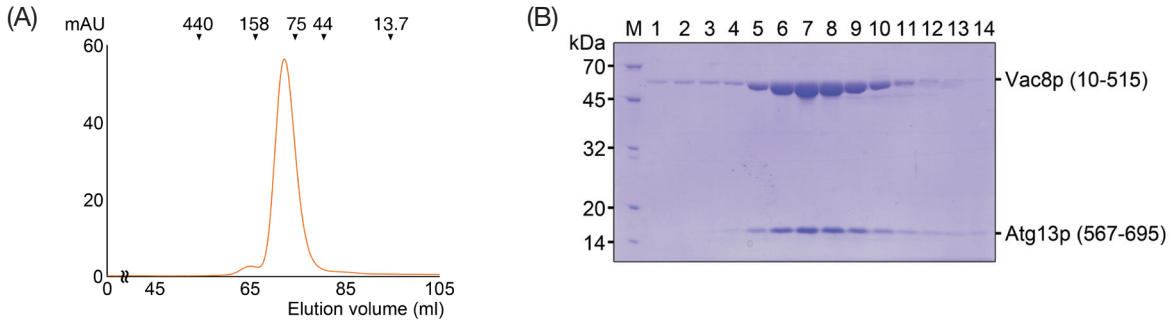

FIGURE 1 | Purification of Vac8p-Atg13p complex in *E. coli* expression system. (A) Elution profile of size-exclusion chromatography of Vac8p-Atg13p complex. Indicated protein standard markers are ferritin, 440kDa; aldolase, 158kDa; conalbumin, 75kDa; ovalbumin, 44kDa; and ribonuclease A, 13.7 kDa, (B) SDS-PAGE analysis of elution fractions from size-exclusion chromatography. Lane M represents molecular-weight marker, and lanes 1-14 indicate the fractions of elution volume from 62.5ml to 83.5ml.

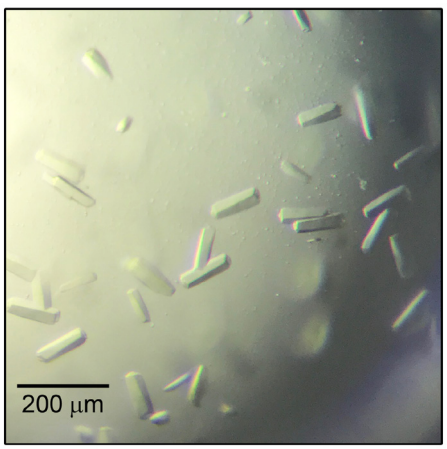

FIGURE 2 | Crystals of Vac8p-Atg13p complex. Crystals of the *S. cerevisiae* Vac8p-Atg13p complex grown in 25% (v/v) PEG 400, 100 mM Tris pH 8.5, 2% (v/v) Ethylene glycol, 2% (w/v) PEG 3350, 1.5% (w/v) PEG 20000, 5 mM DTT at 293K.

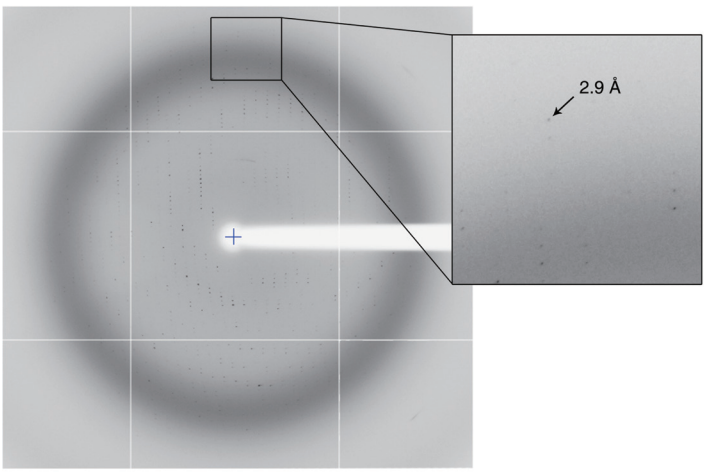

FIGURE 3 | Representative diffraction image of single crystal of Vac8p-Atg13p complex. The diffraction image was obtained using a synchrotron-radiation source. The resolution limit is highlighted with an arrow in the close-up view.

TABLE 3 | Crystallization

Method	Hanging drop vapor diffusion
Plate type	24-well plate, Hampton Research
Temperature (K)	293
Protein concentration (mg ml^{-1})	9
Buffer composition of protein solution	25mM Tris, pH 7.5, 150mM NaCl, 5mM DTT
Composition of reservoir solution	25% (v/v) PEG 400, 100mM Tris pH 8.5, 2% (v/v) Ethylene glycol, 2% (w/v) PEG 3350, 1.5% (w/v) PEG 20000, 5mM DTT
Volume and ratio of drop	2 μl, 1:1
Volume of reservoir (μl)	500

a HiTrap chelating column (GE Healthcare), and then eluted with a buffer containing 25 mM sodium phosphate, pH 7.8, 300 mM NaCl and 400 mM imidazole. His_6-tag of Atg13p and GST of Vac8p were removed by treating TEV and PreScission proteases to a molar ratio protein:protease of 50:1 and 100:1, respectively. Proteins were dialyzed overnight against buffer comprising 25 mM Tris-Cl (pH 7.8), 150 mM NaCl and 5 mM β-mercaptoethanol, and were applied to a 2nd round of Ni^{2+}-IMAC and GST affinity chromatography to remove cleaved tags (His_6-tag and GST) and non-cleaved proteins. Proteins were further purified using size exclusion chromatography (SEC) with HiLoad 16/60 Superdex 200 column (GE Healthcare) equilibrated with buffer containing 25 mM Tris-Cl (pH 7.5), 150 mM NaCl and 5 mM DTT. Homogeneously pooled protein solution was concentrated to 9 mg/ml, and stored at -80°C until use.

Crystallization

For crystallization of Vac8p-Atg13p com-plex, initial crystallization screens were carried out using sitting-drop vapor diffusion method, by mixing

TABLE 4 | Data collection and processing statistics

X-ray source	PAL 5C
Wavelength (Å)	0.97949
Temperature (K)	100
Detector	ADSC Quantum 315r
Crystal-to-detector distance (mm)	300
Rotation range per image (°)	1
Total rotation range (°)	110
Exposure time per image (s)	1
Space group	$P2_12_12_1$
a, b, c (Å)	62.7, 92.4, 139.9
α, β, γ (°)	90, 90, 90
Resolution range (Å)	50.0-2.90 (2.95-2.90)
Total number of reflections	59423
Number of unique reflections	17745
Completeness (%)	95.2 (86.9)
$I / \sigma(I)$	11.27 (1.86)
R_{merge} (%)	12.0 (43.5)
High resolution shell CC1/2	0.496
Redundancy	3.3 (2.8)
Number of molecules in asymmetric unit	1
V_M (Å^3/Da)	2.92
Solvent contents (%)	57.8

*Values in parentheses are for the highest resolution shell.

equal volumes (0.2 µl) of protein solution with commercially available crystallization screen kits including Wizard (Emerald BioSystems), Structure Screen (Molecular Dimensions), Crystal Screen, Grid Screen and MembFac (Hampton Research) using nano-liter pipetting robot (Mosquito, TTP Labtech) at 293K. Crystals were grown in 25% (v/v) PEG 400, 100 mM Tris pH 8.5, 5 mM DTT and after five days, crystals reached a maximum length of 0.02 x 0.02 x 0.5 mm. To obtain diffraction quality crystals, crystallization conditions were optimized by changing pH and adding precipitants such as alcohols, salts and additive screening kits (Hampton Research). The final optimized reservoir solution was comprised of 25% (v/v) PEG 400, 100 mM Tris pH 8.5, 2% (v/v) Ethylene glycol, 2% (w/v) PEG 3350, 1.5% (w/v) PEG 20000 and 5 mM DTT (Table 3). Prior to data collection, harvested crystals were transferred to the reservoir solution supplemented with 30% (v/v) PEG 400 as a cryoprotectant, and flash-frozen in liquid nitrogen.

X-ray data collection and processing

X-ray diffraction data were collected at 100K at the 5C beamline of Pohang Accelerator Laboratory (Pohang, Republic of Korea) at a wavelength of 0.97949 Å (Park et al., 2017). ADSC Quantum 315r detector was used for data collection. Crystals of Vac8p-Atg13p complex diffracted to a maximum of 2.9 Å resolution and belong to the space group $P2_12_12_1$ with a solvent content of 57.8%. Complete diffraction datasets were processed, integrated, and scaled using HKL2000 (Otwinowski and Minor, 1997). Data collection statistics are summarized in Table 4.

CONFLICT OF INTEREST

All authors declare no conflict of interest.

ACKNOWLEDGEMENTS

We thank the staff at the 5C beamline at the Pohang Accelerator Laboratory (PAL) for assistance with synchrotron facilities. This research was supported by grants from the Cell Logistics Research Center (2016R1A5A1007318) from the National Research Foundation of Korea.

Original Submission: Aug 27, 2017
Revised Version Received: Sep 9, 2017
Accepted: Sep 9, 2017

REFERENCES

Funakoshi, T., Matsuura, A., Noda, T., and Ohsumi, Y. (1997). Analyses of APG13 gene involved in autophagy in yeast, Saccharomyces cerevisiae. *Gene* **192**, 207-213.

Jeong, H., Park, J., Kim, H.I., Lee, M., Ko, Y.J., Lee, S., Jun, Y., and Lee, C. (2017). Mechanistic insight into the nucleus-vacuole junction based on the Vac8p-Nvj1p crystal structure. *Proc Natl Acad Sci U S A* **114**, E4539-E4548.

Klionsky, D.J. (1992). Aminopeptidase I of Saccharomyces cerevisiae is localized to the vacuole independent of the secretory pathway. *J Cell Biol* **119**, 287-299.

Klionsky, D.J., Herman, P.K., and Emr, S.D. (1990). The fungal vacuole: composition, function, and biogenesis. *Microbiol Rev* **54**, 266-292.

Ishikawa, K., Catlett, N.L., Novak, J.L., Tang, F., Nau, J.J., and Weisman, L.S. (2003). Identification of an organelle-specific myosin V receptor. *J Cell Biol* **160**, 887-897.

Matthews, B.W. (1968). Solvent content of protein crystals. *J Mol Biol* **33**, 491-497.

Otwinowski, Z., and Minor, W. (1997). [20] Processing of X-ray diffraction data collected in oscillation mode. *Methods Enzymol* **276**, 307-326.

Park, S.Y., Ha, S.C., and Kim, Y.G. (2017). The Protein Crystallography Beamlines at the Pohang Light Source II. *Biodesign* **5**, 30-34.

Riezman, H. (1985). Endocytosis in yeast: Several of the yeast secretory mutants are defective in endocytosis. *Cell* **40**, 1001-1009.

Roberts, P., Moshitch-Moshkovitz, S., Kvam, E., O'Toole, E., Winey, M., and Goldfarb, D.S. (2003). Piecemeal microautophagy of nucleus in Saccharomyces cerevisiae. *Mol Biol Cell* **14**, 129-141.

Scott, S.V., Nice, D.C., 3rd, Nau, J.J., Weisman, L.S., Kamada, Y., Keizer-Gunnink, I., Funakoshi, T., Veenhuis, M., Ohsumi, Y., and Klionsky, D.J. (2000). Apg13p and Vac8p are part of a complex of phosphoproteins that are required for cytoplasm to vacuole targeting. *J Biol Chem* **275**, 25840-25849.

Takeshige, K., Baba, M., Tsuboi, S., Noda, T., and Ohsumi, Y. (1992). Autophagy in yeast demonstrated with proteinase-deficient mutants and conditions for its induction. *J Cell Biol* **119**, 301-311.

Tang, F., Kauffman, E.J., Novak, J.L., Nau, J.J., Catlett, N.L., and Weisman, L.S. (2003). Regulated degradation of a class V myosin receptor directs movement of the yeast vacuole. *Nature* **422**, 87-92.

Tewari, R., Bailes, E., Bunting, K.A., and Coates, J.C. (2010). Armadillo-repeat protein functions: questions for little creatures. *Trends Cell Biol* **20**, 470-481.

Torggler, R., Papinski, D., Brach, T., Bas, L., Schuschnig, M., Pfaffenwimmer, T., Rohringer, S., Matzhold, T., Schweida, D., Brezovich, A., and Kraft, C. (2016). Two Independent Pathways within Selective Autophagy Converge to Activate Atg1 Kinase at the Vacuole. *Mol Cell* **64**, 221-235.

Wang, Y.X., Catlett, N.L., and Weisman, L.S. (1998). Vac8p, a Vacuolar Protein with Armadillo Repeats, Functions in both Vacuole Inheritance and Protein Targeting from the Cytoplasm to Vacuole. *J Cell Biol* **140**, 1063-1074.

